

# Constraining self-interacting dark matter with the full dataset of PandaX-II

Jijun Yang<sup>1</sup>, Abdusalam Abdukerim<sup>1</sup>, Wei Chen<sup>1</sup>, Xun Chen<sup>1,2</sup>, Yunhua Chen<sup>3</sup>, Chen Cheng<sup>4</sup>, Xiangyi Cui<sup>5</sup>, Yingjie Fan<sup>6</sup>, Deqing Fang<sup>7</sup>, Changbo Fu<sup>7</sup>, Mengting Fu<sup>8</sup>, Lisheng Geng<sup>9,10</sup>, Karl Giboni<sup>1</sup>, Linhui Gu<sup>1</sup>, Xuyuan Guo<sup>3</sup>, Ke Han<sup>1</sup>, Changda He<sup>1</sup>, Shengming He<sup>3</sup>, Di Huang<sup>1</sup>, Yan Huang<sup>3</sup>, Ran Huo<sup>11</sup>, Yanlin Huang<sup>12</sup>, Zhou Huang<sup>1</sup>, Xiangdong Ji<sup>13</sup>, Yonglin Ju<sup>14</sup>, Shuaijie Li<sup>5</sup>, Qing Lin<sup>15,16</sup>, Huaxuan Liu<sup>14</sup>, Jianglai Liu<sup>\*1,2,5</sup>, Xiaoying Lu<sup>17,18</sup>, Wenbo Ma<sup>1</sup>, Yugang Ma<sup>7</sup>, Yajun Mao<sup>8</sup>, Yue Meng<sup>1,2</sup>, Nasir Shaheed<sup>17,18</sup>, Kaixiang Ni<sup>1</sup>, Jinhua Ning<sup>3</sup>, Xuyang Ning<sup>1</sup>, Xiangxiang Ren<sup>17,18</sup>, Changsong Shang<sup>3</sup>, Guofang Shen<sup>9</sup>, Lin Si<sup>1</sup>, Andi Tan<sup>13</sup>, Anqing Wang<sup>17,18</sup>, Hongwei Wang<sup>19</sup>, Meng Wang<sup>17,18</sup>, QiuHong Wang<sup>7</sup>, Siguang Wang<sup>8</sup>, Wei Wang<sup>4</sup>, Xiuli Wang<sup>14</sup>, Zhou Wang<sup>1,2</sup>, Mengmeng Wu<sup>4</sup>, Shiyong Wu<sup>3</sup>, Weihao Wu<sup>1</sup>, Jingkai Xia<sup>1</sup>, Mengjiao Xiao<sup>13,21</sup>, Xiang Xiao<sup>4</sup>, Pengwei Xie<sup>5</sup>, Binbin Yan<sup>1</sup>, Yong Yang<sup>†1</sup>, Chunxu Yu<sup>6</sup>, Hai-Bo Yu<sup>‡20</sup>, Jumin Yuan<sup>17,18</sup>, Ying Yuan<sup>1</sup>, Xinning Zeng<sup>1</sup>, Dan Zhang<sup>13</sup>, Tao Zhang<sup>1</sup>, Li Zhao<sup>1</sup>, Qibin Zheng<sup>10</sup>, Jifang Zhou<sup>3</sup>, Ning Zhou<sup>1</sup>, and Xiaopeng Zhou<sup>9</sup>

(PandaX-II Collaboration);

<sup>1</sup> School of Physics and Astronomy, Shanghai Jiao Tong University, MOE Key Laboratory for Particle Astrophysics and Cosmology, Shanghai Key Laboratory for Particle Physics and Cosmology, Shanghai 200240, China;

<sup>2</sup> Shanghai Jiao Tong University Sichuan Research Institute, Chengdu 610213, China;

<sup>3</sup> Yalong River Hydropower Development Company, Ltd., 288 Shuanglin Road, Chengdu 610051, China;

<sup>4</sup> School of Physics, Sun Yat-Sen University, Guangzhou 510275, China;

<sup>5</sup> Tsung-Dao Lee Institute, Shanghai 200240, China;

<sup>6</sup> School of Physics, Nankai University, Tianjin 300071, China;

<sup>7</sup> Key Laboratory of Nuclear Physics and Ion-beam Application (MOE), Institute of Modern Physics, Fudan University, Shanghai 200433, China;

<sup>8</sup> School of Physics, Peking University, Beijing 100871, China;

<sup>9</sup> School of Physics, Beihang University, Beijing 100191, China;

<sup>10</sup> International Research Center for Nuclei and Particles in the Cosmos & Beijing Key Laboratory of Advanced Nuclear Materials and Physics, Beihang University, Beijing 100191, China;

<sup>11</sup> Shandong Institute of Advanced Technology, Jinan 250103, China;

<sup>12</sup> School of Medical Instrument and Food Engineering, University of Shanghai for Science and Technology, Shanghai 200093, China;

<sup>13</sup> Department of Physics, University of Maryland, College Park, Maryland 20742, USA;

<sup>14</sup> School of Mechanical Engineering, Shanghai Jiao Tong University, Shanghai 200240, China;

<sup>15</sup> State Key Laboratory of Particle Detection and Electronics, University of Science and Technology of China, Hefei 230026, China;

<sup>16</sup> Department of Modern Physics, University of Science and Technology of China, Hefei 230026, China;

<sup>17</sup> Key Laboratory of Particle Physics and Particle Irradiation of Ministry of Education, Shandong University, Jinan 250100, China;

<sup>18</sup> Research Center for Particle Science and Technology, Institute of Frontier and Interdisciplinary Science, Shandong University, Qingdao 266237, Shandong, China ;

<sup>19</sup> Shanghai Advanced Research Institute, Chinese Academy of Sciences, Shanghai 201210, China;

<sup>20</sup> Department of Physics and Astronomy, University of California, Riverside, California 92507, USA;

<sup>21</sup> Center of High Energy Physics, Peking University, Beijing 100871, China

---

Self-interacting Dark Matter (SIDM) is a leading candidate proposed to solve discrepancies between predictions of the prevailing cold dark matter theory and observations of galaxies. Many SIDM models predict the existence of a light force carrier that mediate strong dark matter self-interactions. If the mediator couples to the standard model particles, it could produce characteristic signals in dark matter direct detection experiments. We report searches for SIDM models with a light mediator using the full dataset of the PandaX-II experiment, based on a total exposure of 132 tonne-days. No significant excess over background is found, and our likelihood analysis leads to a strong upper limit on the dark matter-nucleon coupling strength. We further combine the PandaX-II constraints and those from observations of the light element abundances in the early universe, and show that direct detection and cosmological probes can provide complementary constraints on dark matter models with a light mediator.

**dark matter, direct detection, self-interacting dark matter**

**PACS number(s):** 95.35.+d, 29.40.Mc, 29.40.Gx

## 1 Introduction

A fundamental question beyond the standard model of particle physics concerns the nature of dark matter, which makes up over 80% of the mass in the universe. In the prevailing theory, dark matter consists of cold and collisionless particles, for example, in the form of weakly interacting massive particles (WIMPs) [1]. This theory is extremely successful in explaining large-scale structure of the universe [2]. But it has difficulties in accommodating observations of dark matter distributions in galaxies, see [3, 4]. A promising solution is to consider self-interacting dark matter (SIDM) [5, 6], where dark matter particles have strong self-interactions. Studies show that SIDM can change the inner halo structure and provide better agreement with galactic observations, see [3] for a review and references therein.

In many particle physics realizations of SIDM, a light force carrier ( $\phi$ ) is introduced to mediate the self-interactions and its typical mass is  $\sim 10$  MeV [3]. When  $\phi$  couples to the standard model particles, it can lead to characteristic signals in direct detection experiments such as PandaX-II [7]. Compared to traditional WIMP searches, the SIDM signal spectrum is peaked more towards low energies since the mediator mass is comparable to the momentum transfer in nuclear recoils [8, 9]. For the same reason, direct searches can put a strong constraint on the mixing parameter between the two sectors. In [10], we reported searches for dark matter-nucleon interactions mediated by a light mediator using PandaX-II data with an exposure of 54 tonne-days, and derived an upper limit on the mixing parameter  $\lesssim 10^{-10}$ . The XENON collab-

oration also carried out searches for a similar model [11].

In this work, we perform searches for dark matter models with a light mediator using the full dataset of PandaX-II, corresponding to a total exposure of 132 tonne-days, and find no significant excess over background. We interpret the results in terms of a well-motivated SIDM model that has been shown to explain dark matter distributions from dwarf galaxies to galaxy clusters [6, 12]. In addition, we combine the PandaX-II constraints and those from observations of the light element abundances in the early universe [13, 14], and show that they provide a complementary test of the self-interacting nature of dark matter. In particular, our results indicate that the dark sector needs to be colder than the visible sector in the early universe for dark matter masses ranging from  $\sim 10$  GeV to 200 GeV.

## 2 Experiment and Method

PandaX-II is a dark matter direct detection experiment, located in China Jinping underground laboratory. Its central apparatus is a dual-phase xenon time projection chamber, containing 580 kg liquid xenon in the sensitive volume. Energy deposit from particles interacting with liquid xenon results in prompt scintillation lights ( $S1$  signal) and ionization electrons which are drifted up to gaseous xenon and produce delayed second scintillation lights ( $S2$  signal). Both signals are recorded in one trigger window (one event). More detailed descriptions of the experiment can be found in [15–17].

As in [10], we first consider a general case where the in-

---

\*Spokesperson: jianglai.liu@sjtu.edu.cn

†Corresponding author: yong.yang@sjtu.edu.cn

‡Corresponding author: haiboyu@ucr.edu

teraction between dark matter and nucleon is mediated by a force carrier,  $\phi$ . If we further assume equal effective couplings to proton and neutron as in the standard WIMP search, the general form of the dark matter-nucleon elastic scattering cross section can be parametrized as [8]

$$\sigma(q^2)_{\chi N} = \sigma|_{q^2=0} A^2 \left( \frac{\mu}{\mu_p} \right)^2 \frac{m_\phi^4}{(m_\phi^2 + q^2)^2} F^2(q^2), \quad (1)$$

where  $\sigma|_{q^2=0}$  is the dark matter-nucleon cross section in the limit of zero momentum transfer ( $q^2 = 0$ ),  $A$  is the mass number of the nucleus,  $\mu$  ( $\mu_p$ ) is the dark matter-nucleus (nucleon) reduced mass,  $m_\phi$  is the mediator mass, and  $F(q^2)$  is the nuclear form factor [18]. We can see that  $\sigma_{\chi N}$  is momentum-dependent and it approaches the standard WIMP case when  $m_\phi \gg q$ . The corresponding differential recoil rate is [19]

$$\frac{dR}{dE} = \frac{\sigma(q^2)_{\chi N} \rho}{2m_\chi \mu^2} \int_{v \geq v_{\min}} d^3v v f(v, t), \quad (2)$$

where  $\rho = 0.3 \text{ GeV/cm}^3$  is the local dark matter density,  $m_\chi$  is the dark matter mass,  $f(v, t)$  is the time-dependent velocity distribution relative to the detector, and  $v_{\min}$  is the minimum velocity that results in a recoil energy of  $E$ . The event rate is calculated based on the standard isothermal halo model [19, 20] with a circular velocity of 220 km/s, a galactic escape velocity of 544 km/s, and an average Earth velocity of 245 km/s.

We select dark matter candidate events in the same way as in the final WIMP search of PandaX-II [21]. The main event selection requires one  $S1$  signal in the range of 3 photoelectron (PE) and 45 PE, and one  $S2$  signal in the range of 100 PE (uncorrected) and 10000 PE. Figure 1 shows the distribution of the selected events in the  $S1 - \log_{10}(S2/S1)$  plane. The majority of events are distributed in the band of  $1.5 < \log_{10}(S2/S1) < 2.5$ , which are dominated by electron recoil backgrounds. Some are in the region  $\log_{10}(S2/S1) < 1.5$  and  $S1 < 20$ , and they are mostly from surface events; see [21] for details. No significant excess events in data was observed above the background prediction. Expected dark matter yields are estimated using the above recoil event rate and the updated NEST simulation framework [22]. Parameters used in the simulation, such as the light and charge yield, are tuned against the PandaX-II calibration data. Measured experimental efficiencies are also applied. Figure 1 also shows that the light-mediator model and the traditional WIMP model have different signal regions due to the  $m_\phi$  dependence of the recoil energy spectrum.

For statistical analysis, we follow the same construction of test statistics as in Ref. [21] which is based on profile likelihood ratio. Then the standard  $CL_{s+b}$  approach [23] is used to derive the upper limits of  $\sigma|_{q^2=0}$  given dark matter and mediator masses. In the case of strong downward fluctuation, the

reported limits are power-constrained to  $-1\sigma$  of the sensitivity band evaluated from background-only toy data sets.

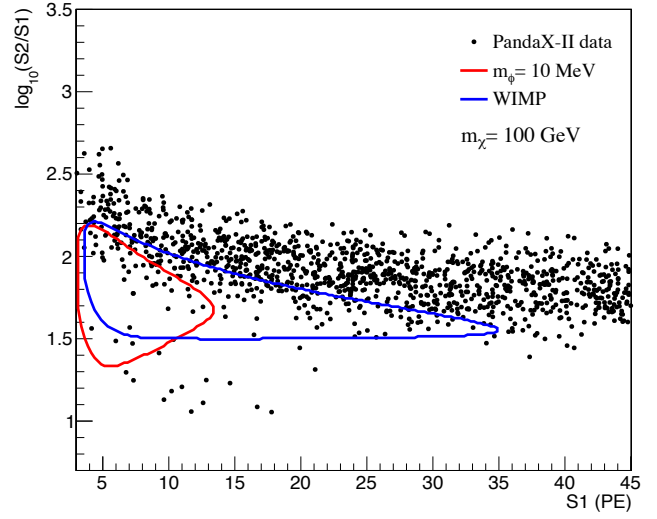


**Figure 1** Selected dark matter candidate events in the  $S1 - \log_{10}(S2/S1)$  plane from the PandaX-II full dataset. The contours contain 68.3% of the expected signals for a dark matter model with a light mediator where  $m_\chi = 100 \text{ GeV}$  and  $m_\phi = 10 \text{ MeV}$  (red) and a WIMP model with the same  $m_\chi$  (blue).

### 3 Results and Discussion

The left panel of Figure 2 shows the 90% CL upper limits on the  $\sigma|_{q^2=0}$  vs the mediator mass for  $m_\chi = 10 \text{ GeV}$  (red) and  $100 \text{ GeV}$  (blue). Overall, they become stronger as the mediator mass increases. For  $m_\phi \gtrsim 100 \text{ MeV}$ , our limits approach those derived for the WIMP case [21], since the momentum transfer becomes negligible in Eq. 1. For  $m_\chi = 10 \text{ GeV}$ , our current exclusion limits are stronger than those found in the 2018 analysis for all  $m_\phi$ . For  $m_\chi = 100 \text{ GeV}$ , both limits are comparable for  $m_\phi \lesssim 30 \text{ MeV}$ . The right panel of Figure 2 shows the limits vs the dark matter mass. In the WIMP case where  $m_\phi = 1 \text{ GeV}$ , the current limits are stronger for  $m_\chi \lesssim 20 \text{ GeV}$ . For  $m_\phi = 1 \text{ MeV}$  and  $10 \text{ MeV}$ , our current limits are stronger for  $m_\chi \lesssim 40 \text{ GeV}$ . Consider  $m_\chi \approx 15 \text{ GeV}$  and  $m_\phi = 10 \text{ MeV}$ , we find  $\sigma|_{q^2=0} < 1.7 \times 10^{-44} \text{ cm}^2$ , which is a factor of 3.9 improvement compared to the 2018 analysis.

To further interpret our search results, we consider a well-motivated SIDM model where dark matter is assumed to be a Dirac fermion and it couples to a vector mediator with a gauge coupling. Refs. [6, 12] show that this model can explain dark matter distributions inferred from spiral galaxies and galaxy clusters, and both mediator mass and gauge coupling can be determined for a range of dark matter masses. Here, we further assume the mediator couples to the photon through kinetic mixing [24],  $\epsilon_\gamma \phi_{\mu\nu} F^{\mu\nu}$ , where  $\epsilon_\gamma$  is the mixing parameter,  $\phi_{\mu\nu}$  and  $F^{\mu\nu}$  are the mediator and photon field

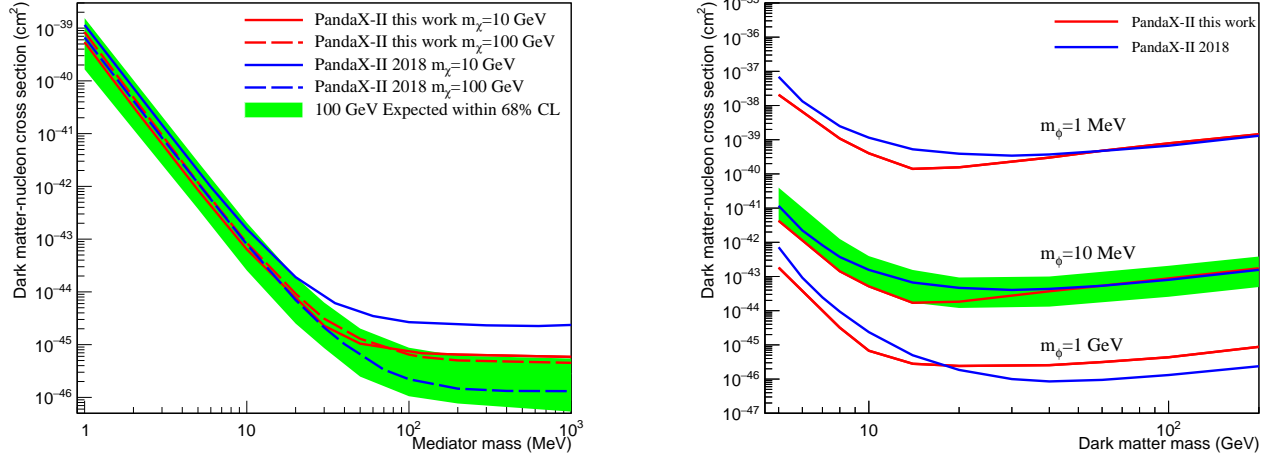


**Figure 2** *Left:* PandaX-II 90% CL upper limits on the zero-momentum dark matter-nucleon cross section vs the mediator mass for  $m_\chi = 10$  GeV (red solid) and 100 GeV (red dashed). *Right:* the limits vs the dark mass  $m_\phi = 1$  MeV, 10 MeV and 1 GeV. In both panels, the green band denotes the  $\pm 1\sigma$  sensitivity for the given model parameters. For comparison, the limits from our previous analysis based on the PandaX-II data release in 2018 [10] are shown (blue).

strengths, respectively. In the  $q^2 = 0$  limit, the dark matter-nucleon cross section is

$$\sigma|_{q^2=0} = \frac{16\pi\alpha_{\text{EM}}\alpha_\chi\mu_p^2}{m_\phi^4} \left[ \frac{\epsilon_\gamma Z}{A} \right]^2, \quad (3)$$

where  $\alpha_{\text{EM}} = 1/137$  and  $\alpha_\chi$  are the fine structure constants in the visible and dark sectors, respectively,  $Z$  is the proton number of the xenon nuclei. In our analysis, we fix  $\alpha_\chi$  to be the best-fit value for given  $m_\chi$  as in [12].

The left panel of Figure 3 shows the PandaX-II constraints in the  $m_\phi$ - $m_\chi$  plane for three representative values of  $\epsilon_\gamma$  (red), together with the favored SIDM parameter region from astrophysical observations (blue), taken from [12]. Our results can constrain a large portion of the SIDM parameter space even for  $\epsilon_\gamma$  being as small as  $2 \times 10^{-11}$ , at which the SIDM model with  $m_\chi \gtrsim 40$  GeV is excluded. The sensitivity further improves as  $\epsilon_\gamma$  increases. For  $\epsilon_\gamma = 10^{-9}$ , the region with  $m_\chi \gtrsim 6$  GeV is excluded. Alternatively, we can derive upper limits in the  $\epsilon_\gamma$ - $m_\phi$  plane for given  $m_\chi$ . This is shown in the right panel of Figure 3 for two representative dark matter masses, 10 GeV and 100 GeV (red).

There are cosmological constraints on the model parameters. In the early universe, the mediator must decay to (almost) massless particles to avoid over-closing the universe [7, 8]. If it decays to standard model particles via the kinetic mixing portal discussed above, the energy injection to the plasma in the early universe may alter the light element abundances and lead to tensions with successful predictions of the standard Big Bang Nucleosynthesis (BBN) scenario. Refs. [13, 14] study BBN constraints and derive lower limits on the mediator lifetime  $\tau_\phi$ , which depend on  $m_\phi$ , the chemical decoupling temperature of  $\phi$  ( $T_{\text{cd}}$ ) and the temperature

ratio when the decoupling occurs ( $\zeta_{\text{cd}}$ ). The last two parameters essentially control the abundance of mediator particles in the early universe. We take their limits for  $T_{\text{cd}} = 10$  GeV,  $\zeta_{\text{cd}} = 1$  and 0.5 from [14], two benchmark examples, and convert them into lower limits on  $\epsilon_\gamma$  for a given  $m_\phi$  via the relation  $\tau_\phi = 3/(\alpha_{\text{SM}}m_\phi\epsilon_\gamma^2)$  [7], which are shown in the right panel of Figure 3 (black). Since higher  $\zeta_{\text{cd}}$  indicates higher  $\phi$  abundances, its lifetime should be shorter to avoid the BBN constraints, resulting in larger  $\epsilon_\gamma$ .

The joint PandaX-II and BBN constraints put interesting tests on the SIDM model. If both sectors have the same temperature as the mediator decouples, i.e.,  $\zeta_{\text{cd}} = 1$ ,  $m_\phi$  has to be higher than 35 MeV and 110 MeV for  $m_\chi = 10$  GeV and 100 GeV, respectively. Thus for the mass range of dark matter we consider, the joint constraints strongly disfavor the SIDM parameter region, as the required mediator mass is  $m_\phi \sim 10$  MeV, denoted by the vertical band of the right panel of Figure 3. On the other hand, for  $\zeta_{\text{cd}} = 0.5$ , the SIDM region is allowed unless  $m_\chi \gtrsim 100$  GeV. Overall, our results show that the dark sector needs to be colder than the visible sector in the early universe.

## 4 Summary

We have used the PandaX-II full dataset to constrain dark matter models with a light mediator and derived upper limits on the dark matter-nucleon elastic scattering cross section. Compared to our previous study based on the PandaX-II data release in 2018, the improvement is significant for dark matter mass below 20 GeV. We interpreted our results in terms of an SIDM model, which is motivated to explain dark matter distributions from dwarf galaxies to galaxy clusters, and ob-

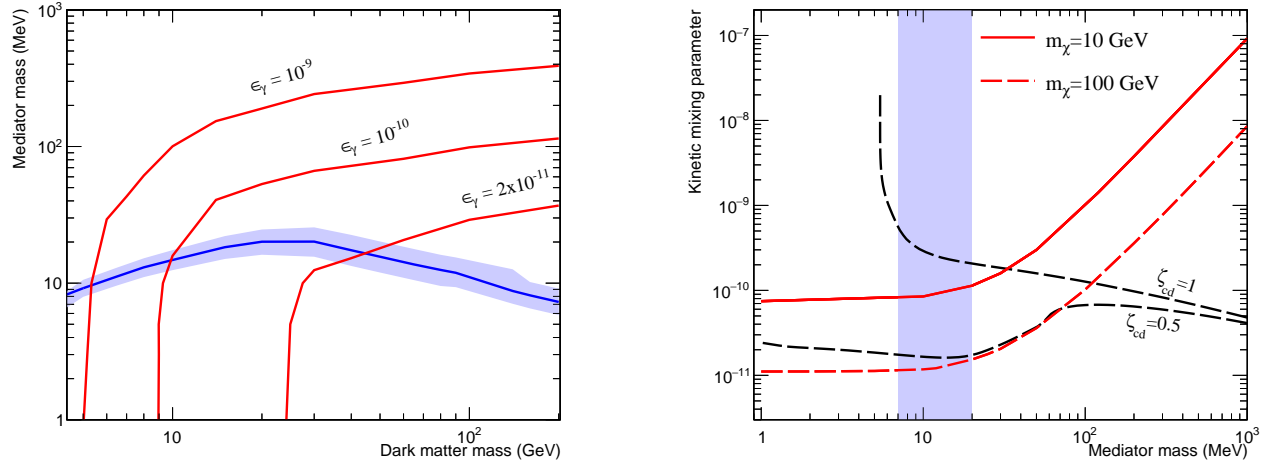


**Figure 3** *Left:* PandaX-II lower limits on the mediator mass for the kinetic mixing parameter  $\epsilon_\gamma = 2 \times 10^{-11}$ ,  $10^{-10}$  and  $10^{-9}$  (red). The blue band denotes the SIDM parameter region favored by observations of dark matter halos from dwarf galaxies to galaxy clusters [12]. *Right:* PandaX-II upper limits on the kinetic mixing parameter for  $m_\chi = 10$  GeV and 100 GeV (red). The vertical band indicates the mediator mass range for SIDM. The black curves indicate lower limits on  $\epsilon_\gamma$  from observations of the light element abundances in the early universe, assuming two benchmark values of the temperature ratio  $\zeta_{cd} = 1$  and 0.5; calculated based on the results in [14].

tained stringent upper limits on the kinetic mixing parameter. We further derived joint constraints on the SIDM model by taking into account *both* PandaX-II searches and observations of the light element abundances in the early universe. Our results demonstrate that direct detection, astrophysical and cosmological observations provide complementary searches for dark matter self-interactions. The next generation of the PandaX experiment, PandaX-4T [25], is expected to improve the detection sensitivity by more than one order of magnitude, and it will further test the particle nature of dark matter.

*This project has been supported by a Double Top-class grant from Shanghai Jiao Tong University, grants from National Science Foundation of China (No 11875190). We thank the Office of Science and Technology, Shanghai Municipal Government and the Key Laboratory for Particle Physics, Astrophysics and Cosmology, Ministry of Education, for important support. This work is supported in part by the Chinese Academy of Sciences Center for Excellence in Particle Physics (CCEPP) and Hongwen Foundation in Hong Kong. Finally, we thank the CJPL administration and the Yalong River Hydropower Development Company Ltd. for indispensable logistical support and other help. HBY acknowledges support from the U. S. Department of Energy under Grant No. de-sc0008541 and the John Templeton Foundation under Grant ID # 61884.*

- 1 Gianfranco Bertone and Dan Hooper and Joseph Silk, Physics Reports. *405*, 279-390 (2005).
- 2 Aghanim, N. et al. (Planck Collaboration), Astron. Astrophys. *641*, A6 (2020).
- 3 Tulin, Sean and Yu, Hai-Bo, Phys. Rept. *730*, 1-57 (2018).
- 4 Bullock, James S. and Boylan-Kolchin, Michael, Ann. Rev. Astron. Astrophys. *55*, 343-387 (2017).
- 5 Spergel, N. David and Paul J. Steinhardt, Phys. Rev. Lett. *84*, 3760-3763 (2000).
- 6 Kaplinghat, Manoj and Tulin, Sean and Yu, Hai-Bo, Phys. Rev. Lett. *116*, 041302 (2016).
- 7 Kaplinghat, Manoj and Tulin, Sean and Yu, Hai-Bo, Phys. Rev. D *89*, 035009 (2014).
- 8 N. Del, Eugenio and Kaplinghat, Manoj and H. B. Yu, JCAP. *10*, 055 (2015).
- 9 Li, Tai and Miao, Sen and Zhou, Yu-Feng, JCAP. *03*, 032 (2015).
- 10 X. X. Ren, et al. (PandaX-II Collaboration), Phys. Rev. Lett. *121*, 021304 (2018).
- 11 Aprile, E. et al. (XENON Collaboration), Phys. Rev. Lett. *123*, 251801 (2019).
- 12 R. Huo, Kaplinghat, Manoj, Z. Pan and H. B. Yu, Phys. Lett. B. *783*, 76-81 (2018).
- 13 Hufnagel, Marco and Schmidt-Hoberg, Kai and Wild, Sebastian, JCAP. *11*, 032 (2018).
- 14 Depta, Paul Frederik and Hufnagel, Marco and Schmidt-Hoberg, Kai, arXiv: 2011.06519.
- 15 A. D. Tan, et al. (PandaX-II Collaboration), Phys. Rev. D *93*, 122009 (2016).
- 16 A. D. Tan, et al. (PandaX-II Collaboration), Phys. Rev. Lett. *117*, 121303 (2016).
- 17 X. Y. Cui, et al. (PandaX-II Collaboration), Phys. Rev. Lett. *119*, 181302 (2017).
- 18 J. D. Lewin and P. F. Smith, Astropart. Phys. *6*, 87-112 (1996).
- 19 C. Savage, G. Gelmini, P. Gondolo and K. Freese, JCAP. *0904*, 010 (2009).
- 20 Smith, Martin C. et al. Mon. Not. R. Astron. Soc. *379*, 755 (2007).
- 21 Q. H. Wang, et al. (PandaX-II Collaboration), Chin. Phys. C. *44*, 125001 (2020).
- 22 M. Szydagis, J. Balajthy, J. Brodsky, et al., Noble element simulation technique v2.0, July 2018.
- 23 Junk, Thomas, Nucl. Instrum. Meth. A. *434*, 435-443 (1999).
- 24 Holdom, Bob, Phys. Lett. *166B*, 196-198 (1986).
- 25 H. G. Zhang, et al. (PandaX-II Collaboration), Sci. China Phys. Mech. Astron. *62*, 31011 (2019).